J. Webster (ed.), *Wiley Encyclopedia of Electrical and Electronics Engineering*


# QUASI-OPTICAL CIRCUITS

In contrast to conventional electronic circuits in which the input and output signals are voltages and currents, quasi-optical circuits have input and output signals that are electromagnetic beams. Quasi-optical circuits use components typically associated with optics, such as lenses, mirrors, and polarizers, but are targeted toward the millimeter- and sub-millimeter-wave regimes of the electromagnetic spectrum between 30 GHz and a few terahertz. This article focuses on *active* quasi-optical circuits used for generating, amplifying, and processing millimeter-wave beams.

Millimeter-wave systems offer a number of advantages over their microwave and optical counterparts. Compared with microwave systems, millimeter-wave systems have wider bandwidth and reduced size and weight. Compared with optical systems, millimeter waves have the advantage of penetrating smoke, fog, and dust. Millimeter-wave applications include high-resolution imaging systems, satellite cross-links, automotive collision avoidance, indoor wireless communications, and identification tagging for tracking inventory.

These applications often exploit the atmospheric absorption characteristics of the millimeter-wave regime (Fig. 1). For example, the attenuation windows are used for long-range communications and radar systems, while the absorption peaks are used for short-range communication systems such as indoor wireless local-area networks and covert battlefield communications.

A major obstacle in developing millimeter-wave systems, however, is the limited power-handling capacity of semiconductor devices in this frequency range. Figure 2 (1) compares the average power of representative solid-state and vacuum electronic devices. While solid-state devices have the advantage of size, weight, reliability, manufacturability, and dc requirements, their power tends to fall off with a $1/f$ to $1/f^2$ frequency dependence.

To take advantage of the benefits of solid-state technology while at the same time meeting system specifications, the power from many individual devices must be added coherently. Although a variety of power combiners based on conventional circuit techniques have been developed (2), they have serious limitations at millimeter-wave frequencies where large numbers of devices must be combined and transmission losses are excessive.

## Quasi-Optical Power Combining

To address this problem, research has concentrated on developing power combiners using quasi-optical methods. Although active quasi-optical techniques have a history dating back several decades, it was Mink's classical paper on quasi-optical power combining (3) that provided the catalyst for the increased research activity in recent years. A quasi-optical power combiner can be likened to a gas-laser system, shown in Fig. 3. Even though each gas molecule contributes just a small portion of the total power in the optical beam, the total power can be quite large. This combining scheme is efficient for two reasons: because of the dense packing of molecules in the system and because the combined power is guided in free space rather than by lossy metal walls.

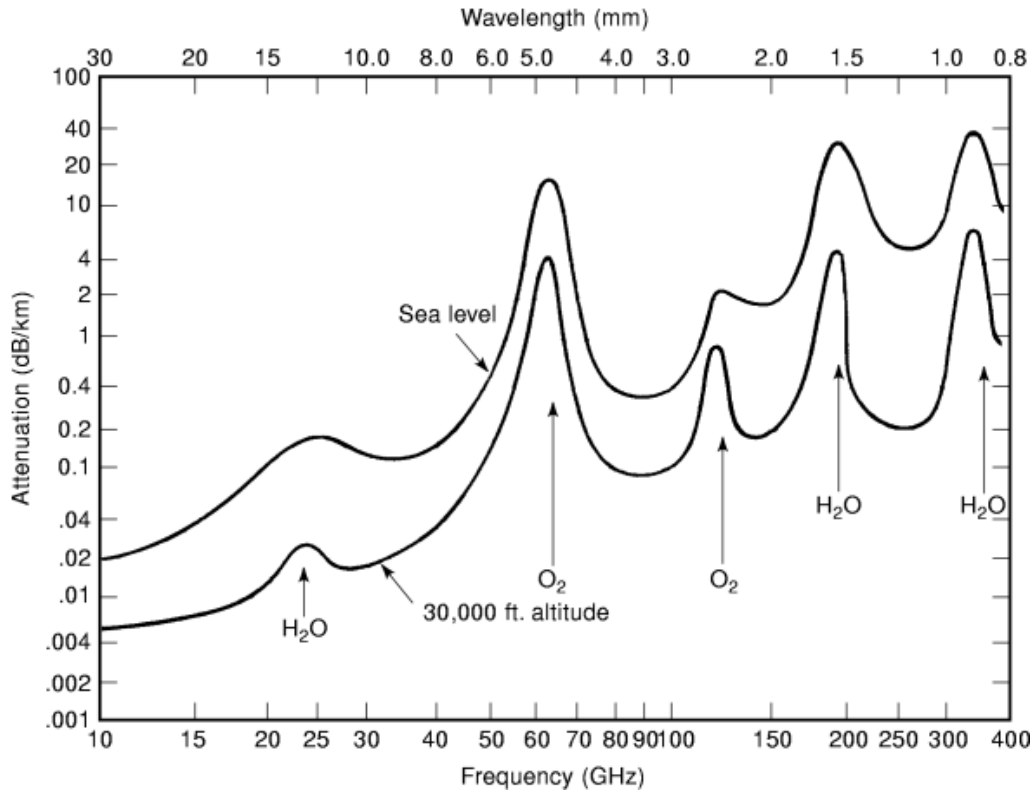


**Fig. 1.** Atmospheric absorption of millimeter waves (horizontal propagation). Attenuation windows occur at 35 GHz, 94 GHz, 140 GHz, and 260 GHz. Absorption peaks occur at 21 GHz, 60 GHz, 119 GHz, and 183 GHz (1).

In a quasi-optical power combiner, an array of solid-state devices is distributed over a planar radiating structure and interacts directly with an electromagnetic beam. The spacing between devices scales with frequency: the higher the frequency, the closer the spacing, and therefore more devices can be packed per unit area. As in the laser, the total output power can be substantial, even though the power from an individual device is small.

Since the publication of Mink's paper, quasi-optical applications have evolved beyond just power generation to more functional circuits such as amplifiers, mixers, phase-shifters, switches, frequency multipliers, modulators, and beam-steerers. All of these quasi-optical circuits share the following advantages:

- The array's unit cell primarily determines the driving-point impedances seen by the active devices, while the output power scales with the total number of devices incorporated. This allows a designer to optimize for gain through the unit cell and to select the array size independently to meet the system power requirement. In many arrays already demonstrated, 100 low-power devices have been spatially power-combined.
- Quasi-optical circuits are compact, lightweight, and amenable to monolithic integration. The antenna is an integral part of the circuit design, which reduces the size of the circuit–antenna module since the feed lines are eliminated. The biasing scheme is also simple, since often all of the devices in the array are biased in parallel.
- The noise from each unit cell is usually uncorrelated, so the noise figure for the array will be no worse than the noise figure of a single device, leading to a high signal-to-noise ratio at the receiver.

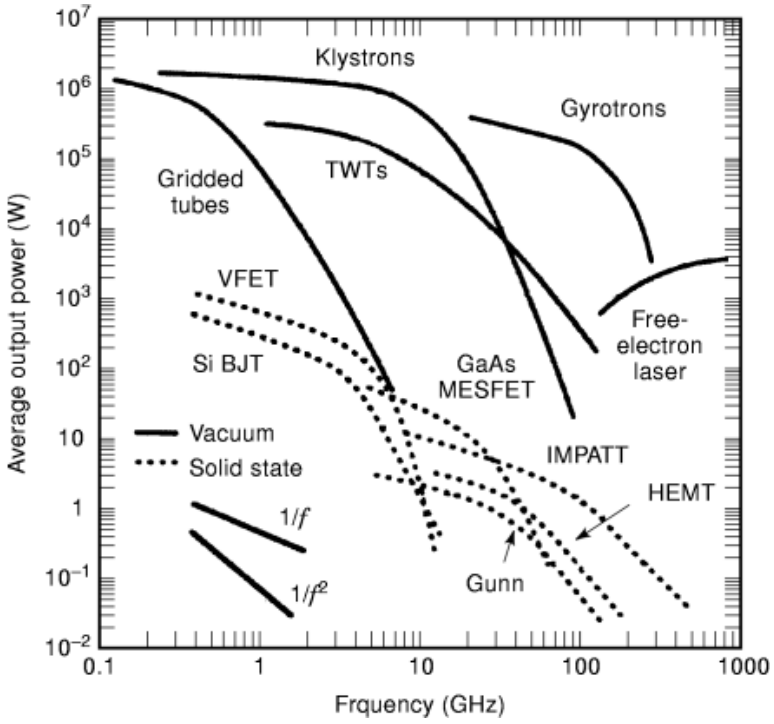


**Fig. 2.** Power-handling capacity of solid-state and vacuum devices (1). The Gunn and impact-ionization-avalanche-transit-time (*IMPATT*) devices are solid-state diodes. The silicon bipolar, metal–semiconductor field-effect transistor (*MESFET*), and high-electron-mobility transistor (*HEMT*) devices are transistors.

- The total output power is a result of combining a large number of devices. Therefore, the reliability of quasi-optical components is high; a fraction of the devices can fail before the component fails, resulting in graceful degradation of the component.

Millimeter-wave power can be generated quasi-optically in three basic ways: by direct conversion of direct current (*dc*) power to radio-frequency (*RF*) power with an oscillator array; by amplifying a low-power source with an amplifier array; or by cascading a low-frequency source with a frequency-multiplier array. Each of these techniques will be discussed in the following sections.

## Oscillators

An oscillator is essentially a device that converts dc power to RF power. In quasi-optical architectures, the RF power must also be radiated efficiently into free space. Quasi-optical oscillators can be divided into two categories: grid oscillators and coupled-oscillator arrays.

**Grid Oscillators.** In the grid approach, solid-state devices are embedded in a metal grating supported by a dielectric substrate (Fig. 4). The horizontal lines of the grid serve as dc bias lines, and the vertical lines as antennas. The mirror, substrate, and grid dimensions are chosen to resonate the devices at the oscillation frequency. The devices are typically spaced a small fraction of a wavelength apart. An oscillation is triggered by any noise or transient on the dc bias. RF currents on the vertical leads cause an electromagnetic wave

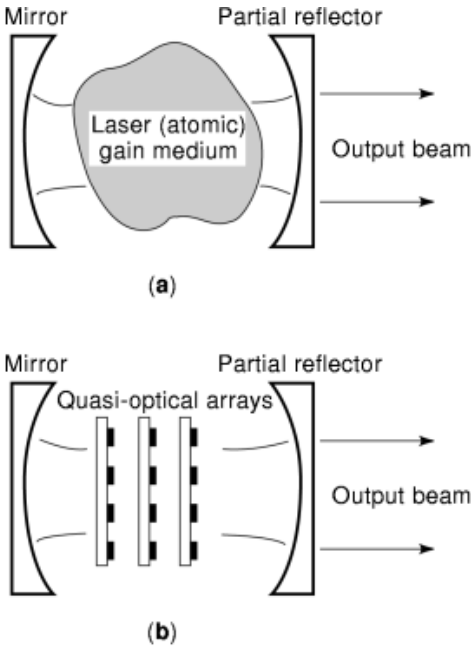


**Fig. 3.** Analogy between a (a) gas laser and (b) quasi-optical power combiner (1).

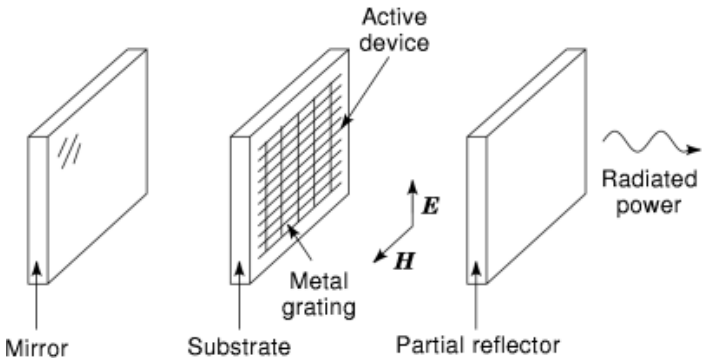


**Fig. 4.** Schematic of a grid oscillator. The radiated power is combined in free space. Courtesy IEEE (10).

to be radiated away from the grid. Feedback from the mirror provides the injection-locking between devices, resulting in a single-frequency, self-locked oscillation.

Grid oscillators have been demonstrated at both microwave and millimeter-wave frequencies, up to 43 GHz (4,5,6,7,8,9,10). Oscillators using up to 100 transistors have been developed, demonstrating the feasibility of large-scale power combining. Active grids can also be cascaded, as demonstrated in Ref. 11, where four transistor grids were placed in a cavity so that the final configuration resembled that of Fig. 3(b). Other cascaded grids include a quasi-optical voltage-controlled oscillator, which was composed of back-to-back transistor and tuning-diode arrays (12).

**Coupled-Oscillator Arrays.** In the grid approach, the oscillator can be interpreted as an active frequency-selective surface with the spacing between devices a small fraction of a wavelength apart. In

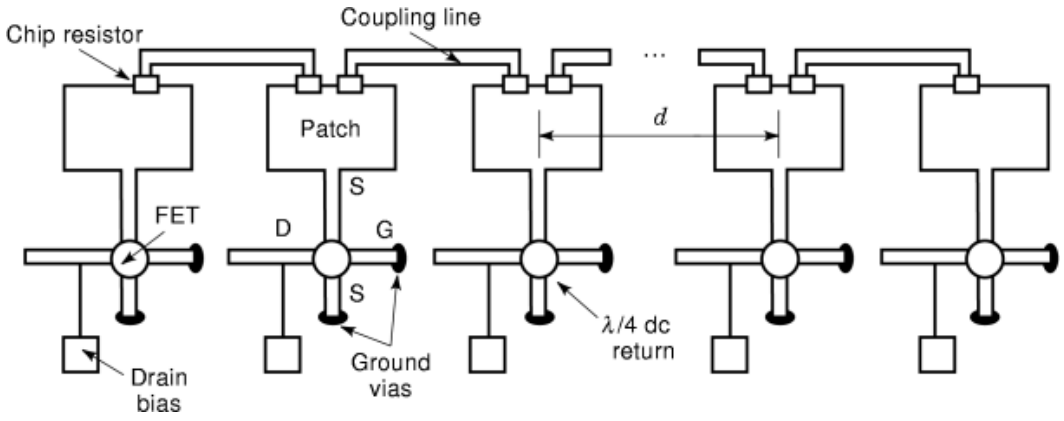


**Fig. 5.** Coupled-oscillator array using patch antennas and field-effect transistors (*FETs*). Courtesy IEEE (24,53).

contrast, in the coupled-oscillator array, each element is independent and contains a conventional planar antenna, and elements are not as closely spaced apart as they are in a grid. Mutual coupling between devices can be enforced using transmission-line interconnections, as shown in Fig. 5. A wide variety of coupled-oscillator arrays have been demonstrated in recent years (13,14,15,16,17,18,19,20,21), owing to the flexibility of this approach.

Electronic steering of the radiated beam, which is important for radar applications, can be accomplished by enforcing a prescribed phase shift between elements in the array. Typically this is done by associating a phase-shifter with each oscillator element; the result is known as a phased array. Two types of steering techniques have been demonstrated in quasi-optical oscillator arrays that do not require individual phase-shifters for each antenna. In the first method, two coherent signals with a predetermined phase shift are injected into two opposite ends of the array (22). The phase shift is divided equally along the chain. In the second method, the constant phase progression is established by detuning the frequencies of the end elements in the array (23). When all of the oscillators are set to the same free-running frequency, the array is uniformly phased and a broadside beam results. When the frequencies of the end elements are slightly detuned from the others, a constant phase progression is established along the array. A scanning range of $-15^\circ$ to $30^\circ$ from broadside was reported for an X-band array (24).

## Amplifiers

Quasi-optical amplifiers have been the object of considerable attention since their development in the early 1990s. Because of their immediate applicability to both military and industrial radar and communications systems, these amplifiers have been the focus of several coordinated academic, government, and industrial research efforts. Several possible amplifier configurations are illustrated in Fig. 6 (25). The amplifier arrays consist of many unit cells, each cell containing input and output antennas connected by an amplifier. The arrays are excited by an input microwave or millimeter-wave beam. The amplified output is re-radiated into free space. The input and output beams are usually orthogonally polarized to provide isolation and thus reduce mutual coupling. Wire-grid polarizers are often used to help confine the signal path to the forward direction. Several amplifier arrays may be cascaded to increase the gain.

Quasi-optical amplifiers are often labeled as being either *grid amplifiers* or *active arrays*. Grid amplifiers have smaller unit cells, typically less than $\lambda_0/4$. A differential transistor pair usually provides the gain. The

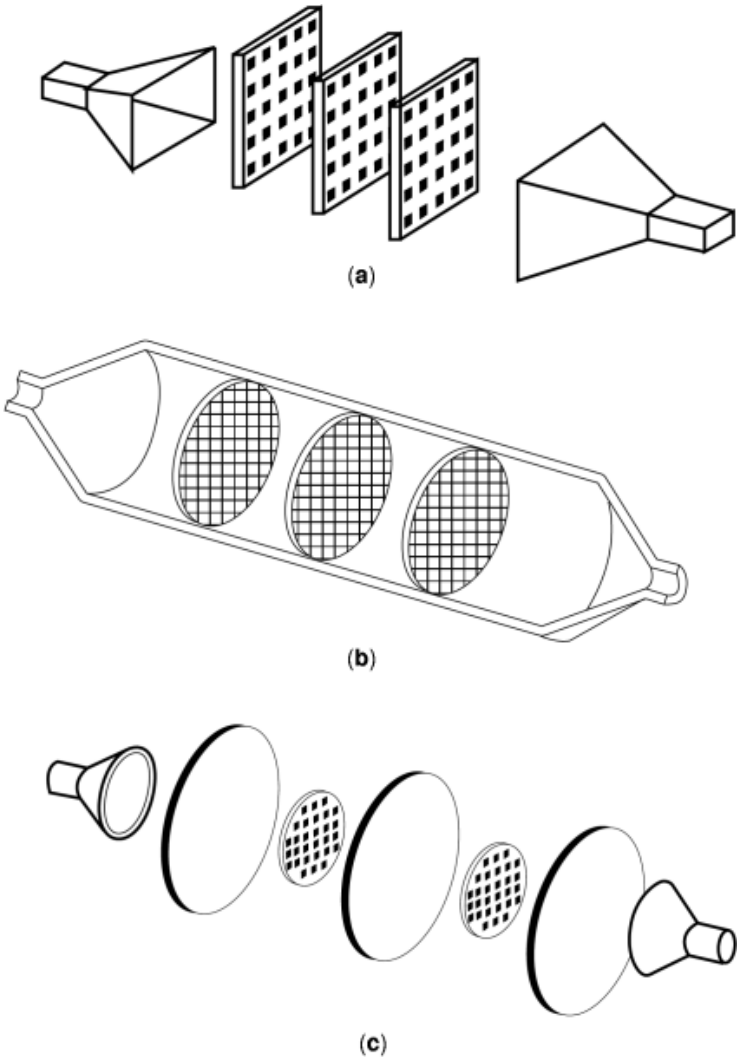


**Fig. 6.** (a) Free-space, (b) waveguide, and (c) lens-focused quasi-optical amplifier configurations (25). Successful amplifiers have been demonstrated using all three configurations (1).

input and output antennas are short dipoles that are strongly coupled due to the close spacing. Grid amplifiers are usually modeled by defining an equivalent waveguide unit cell based on symmetry and then developing a transmission-line equivalent circuit. Active arrays, on the other hand, have larger unit cells, usually near $\lambda_0/2$. Because of the larger cells, multitransistor *MMIC*: monolithic microwave integrated circuit amplifiers can be employed. More conventional resonant slot or patch antennas are often used. Modeling of active arrays is more straightforward because the larger cell reduces coupling between elements. At this point, both the grid-amplifier and active-array approaches have been quite successful.

**Grid Amplifiers.** The first quasi-optical amplifiers were grids developed in the early 1990s by Rutledge and coworkers at the California Institute of Technology (26,27). A unit cell for a 100-element hybrid X-band array using *pHEMT*: pseudomorphic high electron mobility transistor transistors is shown in Fig. 7 (28). A

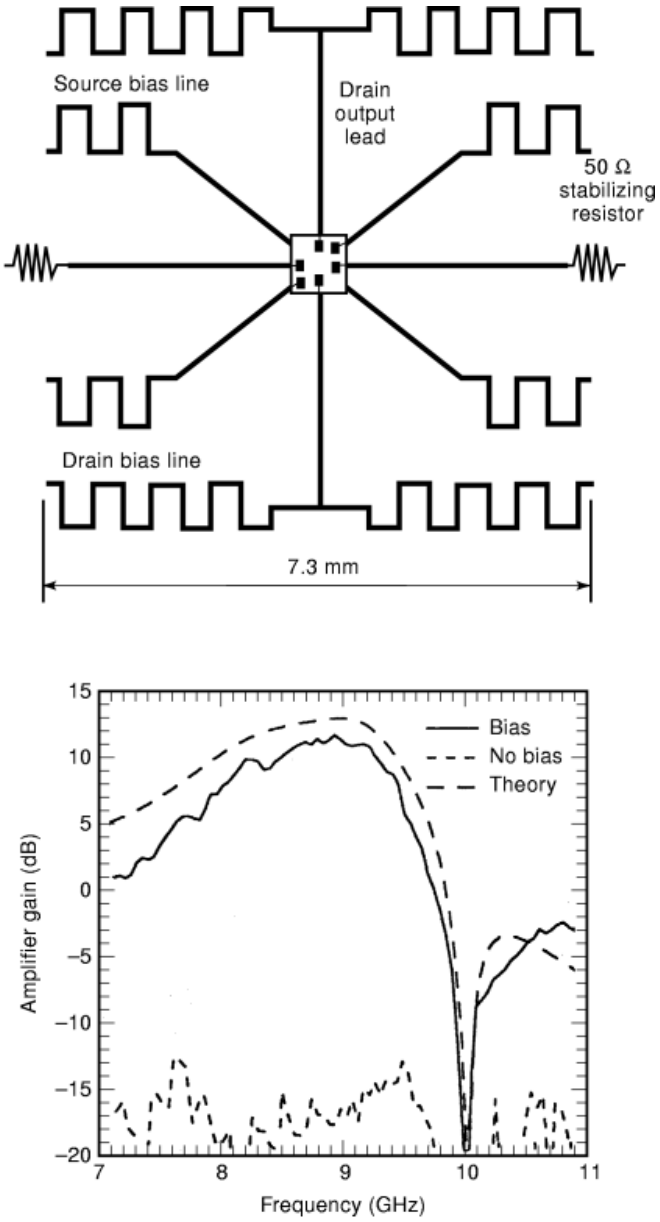


**Fig. 7.** Unit cell and gain of a 100-element pHEMT grid amplifier (28). This grid produced 3.7 W of saturated output power. Courtesy IEEE.

horizontally polarized input beam excites RF currents on the horizontal leads of the grid. These currents drive the gates of the transistor pair in the differential mode. The output currents are redirected along the vertical leads, producing a vertically polarized output beam. Thin meandering lines provide the transistor bias. These bias lines are intended to present a rather high impedance to the input wave. The peak gain is 12 dB at 9 GHz with a 15% 3 dB bandwidth. The minimum noise figure is 3 dB, which is less than 2 dB greater than the

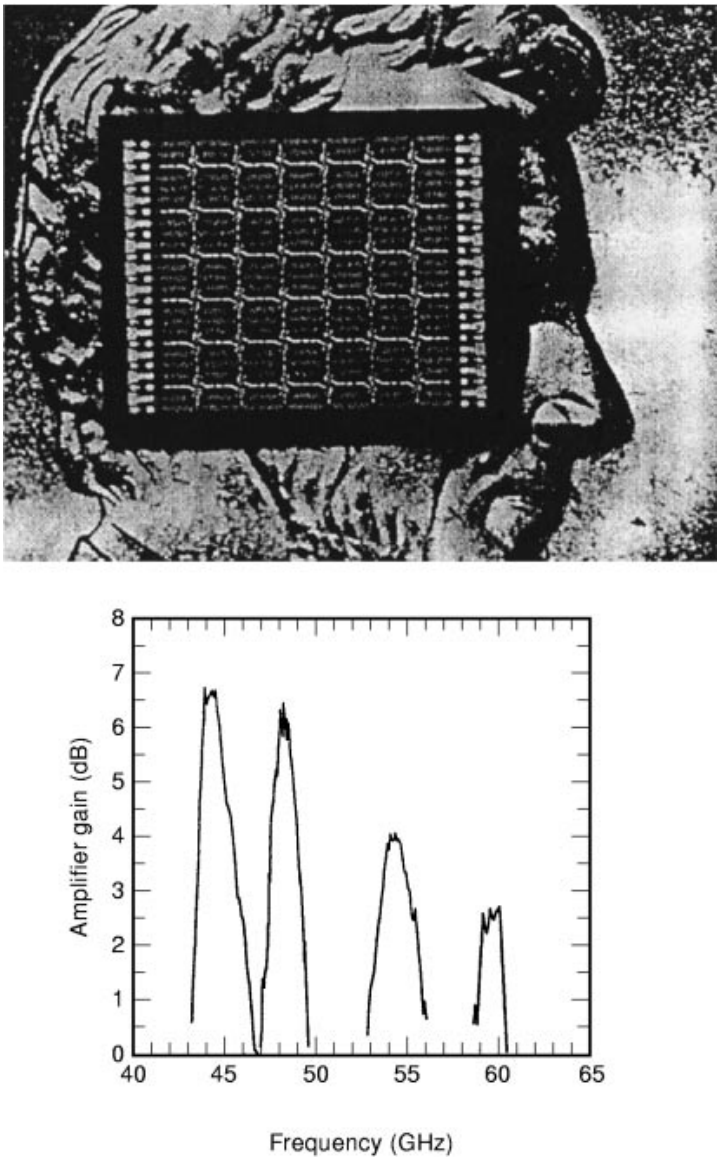


**Fig. 8.** Photograph and gain of a 36-element pHEMT monolithic grid amplifier (30). The unit cell size is 0.52 mm. Courtesy IEEE.

minimum noise figure available from a single HEMT. Finally, this 100-element grid provided 3.7 W of saturated output power.

Grid amplifiers are among the few successful monolithic millimeter-wave quasi-optical amplifiers. A 36-element heterojunction bipolar transistor (HBT) grid produced 5 dB of gain at 40 GHz with a saturated output power of 670 mW (29). Figure 8 shows a photograph of a 36-element pHEMT grid amplifier (30). This amplifier could be tuned to operate at frequencies between 44 GHz and 60 GHz by repositioning the external wire-grid polarizers. Continued efforts are underway to develop monolithic grids further.

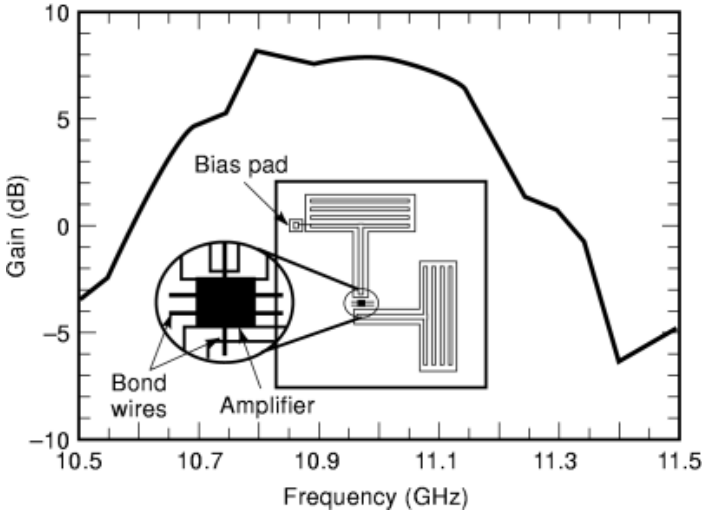


**Fig. 9.** Unit cell and gain of a 16-element active array using folded slot antennas (1,32). The folded slot antennas are designed to match to 50 Ω.

**Active Arrays.** Active-array amplifiers have also been very successful. The approaches vary, but usually involve larger unit cells with more conventional antennas (31,32,33,34,35,36,37,38,39). Amplifiers using back-to-back integrated horn antennas, patch antennas, slot antennas, and probe antennas have been demonstrated. Figure 9 illustrates an approach pursued by York and co-workers at the University of California at Santa Barbara (32). Orthogonally polarized folded slot antennas are used to provide 50Ω input and output feeds. A commercial HBT MMIC amplifier is used as a gain stage. Coplanar waveguide transmission lines connect the amplifier to the antennas. A 16-element array produced about an 8 dB gain at 11 GHz with a 5% bandwidth.

Another very successful approach is the lens–amplifier configuration developed by Popović and others at the University of Colorado (33). Figure 10 shows the idea. Patch antennas are used at the input and output. The two antennas are on opposite sides of a dielectric substrate, isolated by interleaving ground strips. Gain is provided by a single transistor, although multistage amplifiers may also be used. Microstrip lines connect the antennas to the amplifier. Through careful selection of the electrical lengths of these microstrip lines, the array can be designed to focus a plane wave to a spot much like a lens. This particular array demonstrated a peak gain of 8 dB at 9.8 GHz. Other lens amplifiers have also been developed with considerable success (34), including bi-directional amplifiers that can be used for both transmission and reception (35).

Figure 11 illustrates yet another very promising approach developed by York and others (38). MMIC amplifiers are integrated with tapered slot antennas forming an amplifier "card." Several cards are stacked into a conventional metal waveguide to form the active array. This approach has been very successful with an X-band array; a $2 \times 4$ array has achieved 10 dB of gain over the entire waveguide band from 8 GHz to 12 GHz. Furthermore, the array generated 20 W of output power.

Monolithic active-array amplifiers have also shown success in the millimeter-wave band. An array of 112 pHEMT amplifiers achieved a gain of 9 dB at 39 GHz with an output power of 630 mW (39). Researchers are continuing to develop active-array technology for millimeter-wave applications.

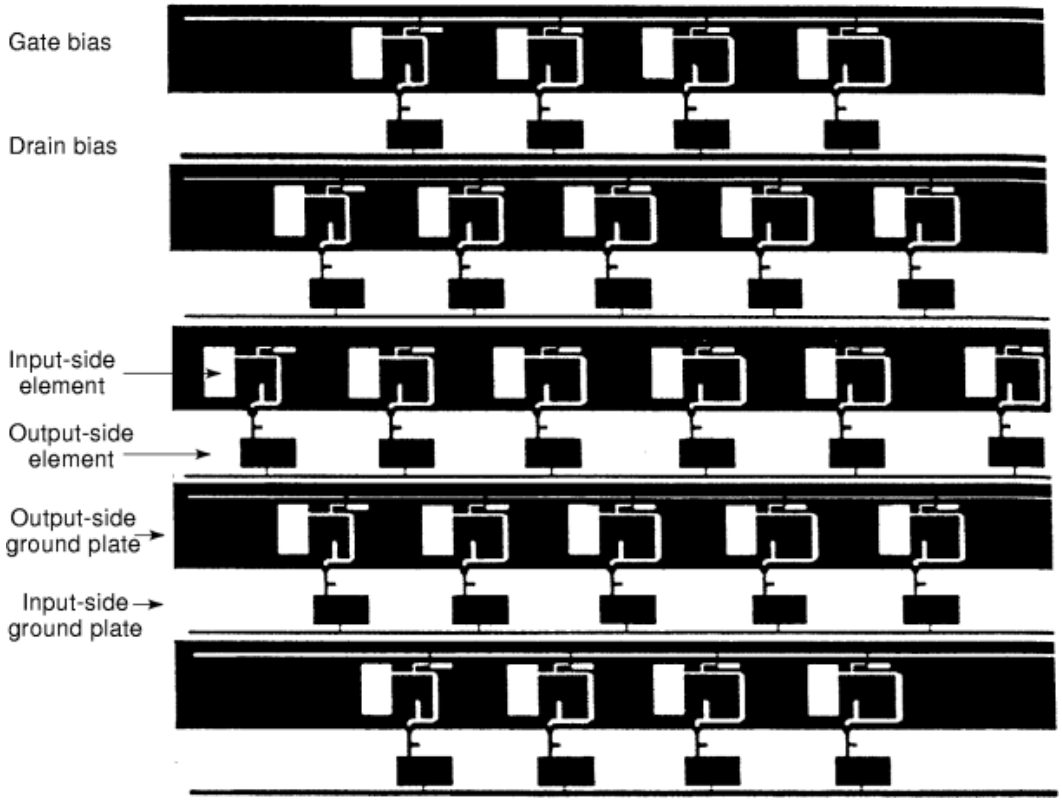


**Fig. 10.** A 24-element lens-amplifier array using patch antennas (33). The input and output patch antennas are on opposite sides of the dielectric substrate, isolated by interleaving ground strips (1).

## Frequency-Conversion and Beam-Control Arrays

Quasi-optical technology shows great promise for many other applications in addition to direct power generation and amplification. Quasi-optical mixers, frequency multipliers, beam switches, and beam-steering components have been investigated. While these components are interesting alone, they are integral components in any quasi-optical transmitter or receiver.

**Frequency-Conversion Arrays.** A quasi-optical grid periodically loaded with diodes will act as a nonlinear surface. When illuminated with an incident beam of radiation, the nonlinearities in the diode array will generate radiation not only at the fundamental frequency, but at higher-order harmonics as well. Diode grids can therefore be used to generate very-high-frequency signals by multiplying a lower fundamental frequency. Luhmann and others at the University of California at Davis have demonstrated a 760-element doubler grid that generated 0.5 W at 66 GHz when illuminated with a 2.5 W input at 33 GHz (40). This group has also reported a 5 W 99 GHz output tripler grid using 3100 diodes (41). Multiplier grids have proven extremely successful at terahertz frequencies; a 144-element doubler produced 5.5 mW output at 1 THz (42–43). This output power is almost 2 orders of magnitude more than that available using competing non-quasi-optical techniques. The terahertz doubler array is shown in Fig. 12. The success of these grids is a testament to the utility of quasi-optics.

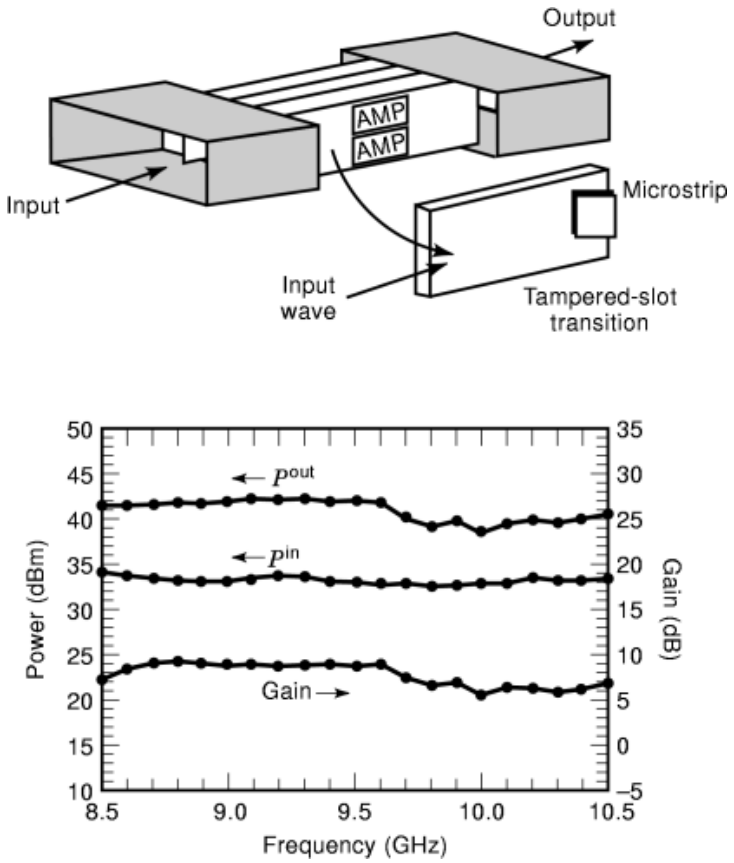


**Fig. 11.** Configuration and gain of an 8-element waveguide active array (38). This array produced 20 W using eight high-power MMICs. Courtesy IEEE.

Diode mixer grids have also been demonstrated. The local oscillator (*LO*) and RF signals illuminate a diode grid quasi-optically. The intermediate-frequency (*IF*) signal is the difference between the RF and LO frequencies. Due to the nature of quasi-optical arrays, the mixer's conversion loss and noise figure are comparable to those of a single-diode microstrip mixer. On the other hand, the array's power-handling capability increases with the number of elements, thereby increasing the dynamic range. A 100-element mixer grid (44) had a third-order intercept nearly 20 dB greater than a single-diode microstrip mixer. This feature makes quasi-optical receivers very attractive for high dynamic range wireless communications applications.

**Beam-Control Arrays.** Diode-grid arrays have also shown promise as beam-control arrays. Quasi-optical phase-shifters (45–46) and switches (46,47,48) are among the many successful beam-control components. Figure 13 shows a millimeter-wave monolithic *p–i–n*-diode switching array (48) developed by Stephan and others. The *p–i–n* diodes act as switches; depending on the dc diode bias, the array will either reflect or transmit an incident beam. This array switched a 94 GHz beam with an insertion loss of 4 dB and an isolation of 22 dB. An array of varactor diodes will behave in a similar way. By varying the varactor bias, and thus the junction capacitance, the phase of a quasi-optical beam can be shifted.

One very intriguing application of quasi-optical phase-shifters is for beam steering. Progressively shifting the phase of an incident beam across the surface of the quasi-optical array will cause the beam to change directions. These quasi-optical beam steerers could one day replace the slow, heavy mechanical systems or the

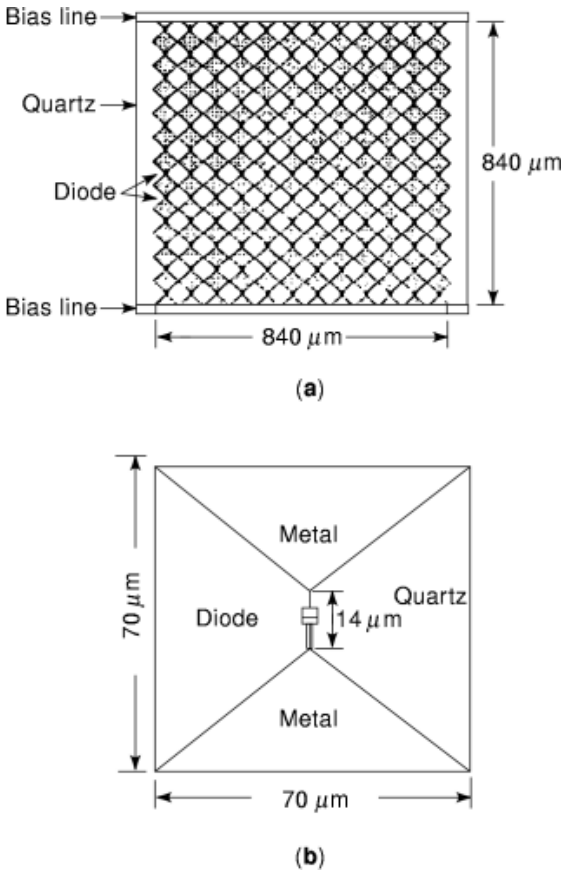


**Fig. 12.** (a) A monolithic terahertz multiplier grid (42) and (b) unit cell detail. This grid produced 5.5 mW at 1 THz. Courtesy IEEE.

complicated phased-array systems used in many radar transmitters. One particularly promising approach is to use tiny microelectromechanical (*MEMS*) switches to provide the phase shift (49) without the parasitic losses associated with millimeter-wave diodes.

## Characterization of Quasi-Optical Arrays

Quasi-optical components are both active circuits and antenna arrays. These components must be characterized with this unique property in mind. Researchers have developed several figures of merit useful for quasi-optical characterization. Gouker (50) has attempted to standardize some of these figures. In this section, characterization of quasi-optical oscillators and amplifiers will be discussed.

**Oscillator Characterization.** Consider the quasi-optical oscillator or transmitter array illustrated in Fig. 14. This array, with active area $A$ and directive gain $G_t$ is located a distance $R$ from a receiving horn antenna with directive gain $G_h$. The quasi-optical array transmits a total power of $P_t$. $\lambda_0$ is the free-space wavelength. The power received by the receiving horn antenna $P_r$ will be given by the Friis transmission

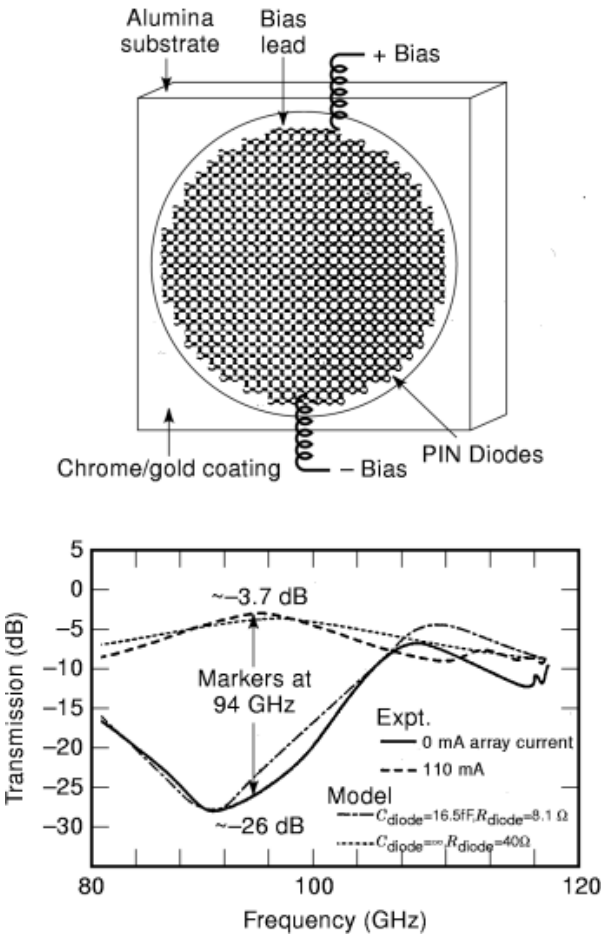


**Fig. 13.** A *p–i–n* diode switch array with measured and modeled transmission loss. Courtesy IEEE (48).

equation:

$$P_r = G_t P_t G_h \left(\frac{\lambda_0}{4\pi R}\right)^2 \qquad (1)$$

$G_h$, $R$, $\lambda_0$ are usually well-known quantities. This measurement directly reveals the array's effective isotropic radiated power (*EIRP*), which is the product of the actual radiated power $P_t$ and the array's directive gain $G_t$:

$$\text{EIRP} = P_t G_t = \frac{P_r}{G_h}\left(\frac{4\pi R}{\lambda_0}\right)^2 \qquad (2)$$

To compute the array's total radiated power, the directive gain $G_t$ must be computed from a complete measurement of the array's three-dimensional radiation pattern. Often, one can estimate the array's directive gain

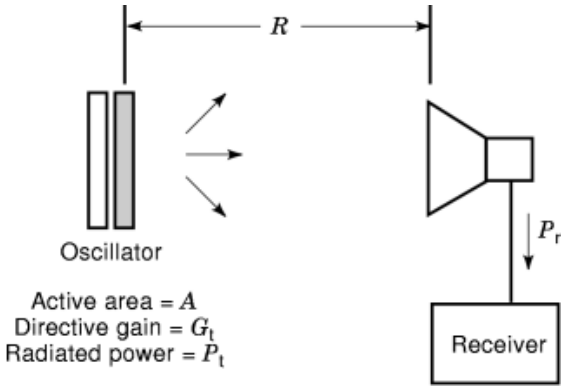


**Fig. 14.** Measurement setup used to characterize a quasi-optical oscillator.

using the active area $A$:

$$G_t \approx \frac{4\pi A}{\lambda_0^2} \tag{3}$$

This approximation is most valid for larger arrays with dimensions of several wavelengths on a side. This gives an estimate of the radiated power from the measured EIRP.

**Amplifier Characterization.** Several techniques have been used to measure the gain of quasi-optical amplifiers. One popular method is a far-field approach shown in Fig. 15. The first step is to calibrate the system. This is done with the two horn antennas co-polarized, as shown in Fig. 15(a). The calibrated power $P_c$ is related to the transmitted power $P_t$ using the Friis transmission equation:

$$\frac{P_c}{P_t} = \left(\frac{G_h \lambda}{4\pi(2R)}\right)^2 \tag{4}$$

where $G_h$ is the directive gain of the transmitting and receiving horn antennas and $R$ is the distance between the amplifier and each horn. Then, the amplifier gain is measured using the setup shown in Fig. 15(b). In this case, the received power is related to the transmitted power by

$$\frac{P_r}{P_t} = \frac{G_h A}{4\pi R^2} G \frac{G_h A}{4\pi R^2} \tag{5}$$

where $G$ is the power gain of the amplifier and $A$ is the physical area of the active array. This allows us to express the amplifier gain as

$$G = \frac{P_r}{P_c}\left(\frac{\lambda R}{2A}\right)^2 \tag{6}$$

This simple formula reveals that the gain of the amplifier can be computed from a relative power measurement and three well-known parameters.

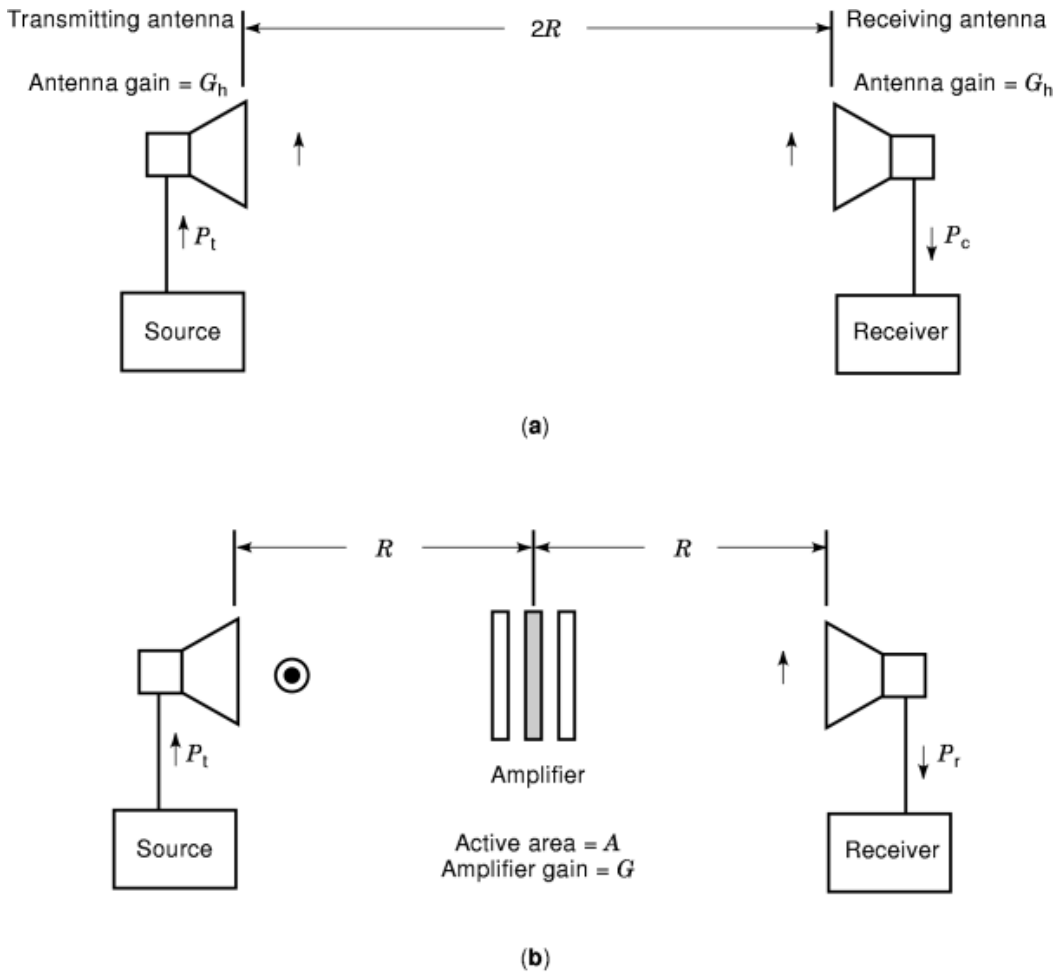


**Fig. 15.** Far-field setup used to measure the gain of a quasi-optical amplifier. (a) The calibration step is performed with the horns co-polarized. (b) The measurement is performed with the horns cross-polarized (1).

Another method used to measure gain is the lens-focused approach shown in Fig. 16. This is a modified version of the quasi-optical reflectometer reported by Gagnon (51). The system is calibrated by placing an absorbing screen at the focal plane, as depicted in Fig. 16(a). The screen has an aperture cut in it, matching the physical area $A$ of the amplifier. The gain is measured in the cross-polarized setup illustrated in Fig. 16(b). For this method, the amplifier gain is simply the ratio of the power received from the grid $P_r$ to the calibration power $P_c$.

A third method of measuring amplifiers involves placing the array in a large, overmoded waveguide (36, 39). Like the lens-focused approach, this method has the advantage of being very straightforward—the gain can be measured directly using a network analyzer. Care must be taken, however, to avoid exciting higher-order waveguide modes. Furthermore, the edges of the overmoded waveguide must be loaded with a dielectric in order to uniformly illuminate the array.

At this point, it should be stressed that the far-field arrangement of Fig. 15 is not how a quasi-optical amplifier is ultimately intended to be used—the high path losses between the grid and the horns would result

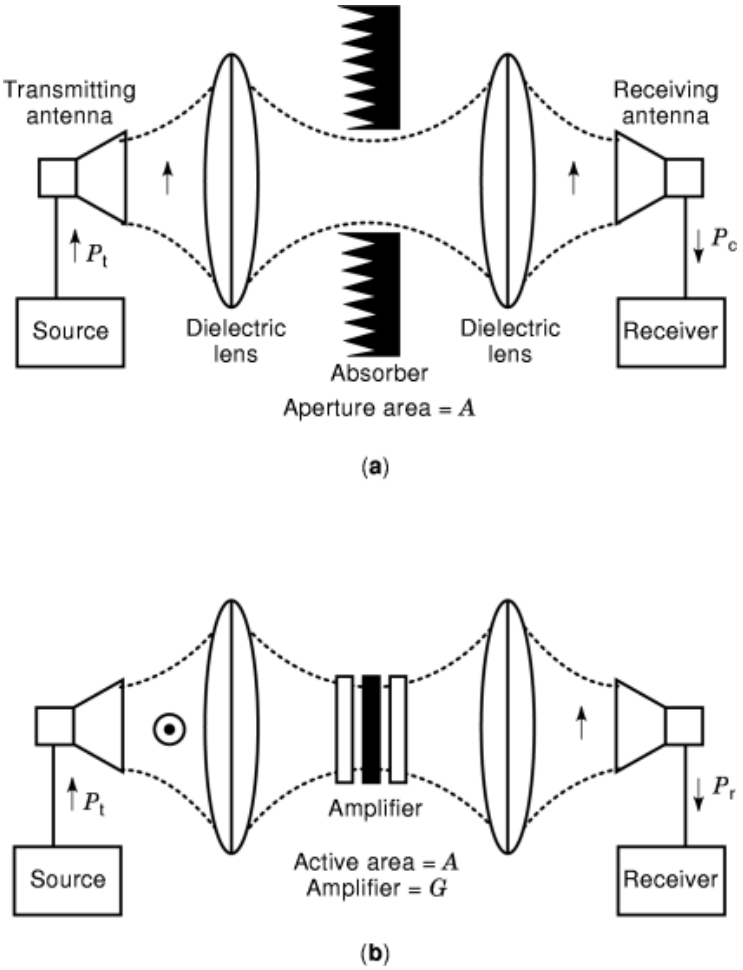


**Fig. 16.** Lens-focused setup used for gain measurement. (a) The calibration step is performed with co-polarized horns and an aperture cut into an absorbing screen. (b) The measurement is performed with the horns cross-polarized (1).

in a very inefficient system. Instead, a quasi-optical amplifier would be employed in a system where the microwave beam is confined, such as in an overmoded waveguide or a lens-focused system like Fig. 16. Much of the diffraction losses are eliminated, possibly resulting in a system with appreciable flange-to-flange gain. On the other hand, the far-field method is simpler to set up in the laboratory, as there are no lenses to focus or align or metal waveguide to machine. Any of the methods should give similar results; the gain of a 100-element HBT grid amplifier was measured using both far-field and lens-focused approaches, with nearly identical results (28).

## Passive Quasi-Optical Components

Passive components are used to characterize the active arrays described above, and are also necessary building blocks for quasi-optical subsystems. Goldsmith (52) summarizes the extensive work on passive quasi-optical

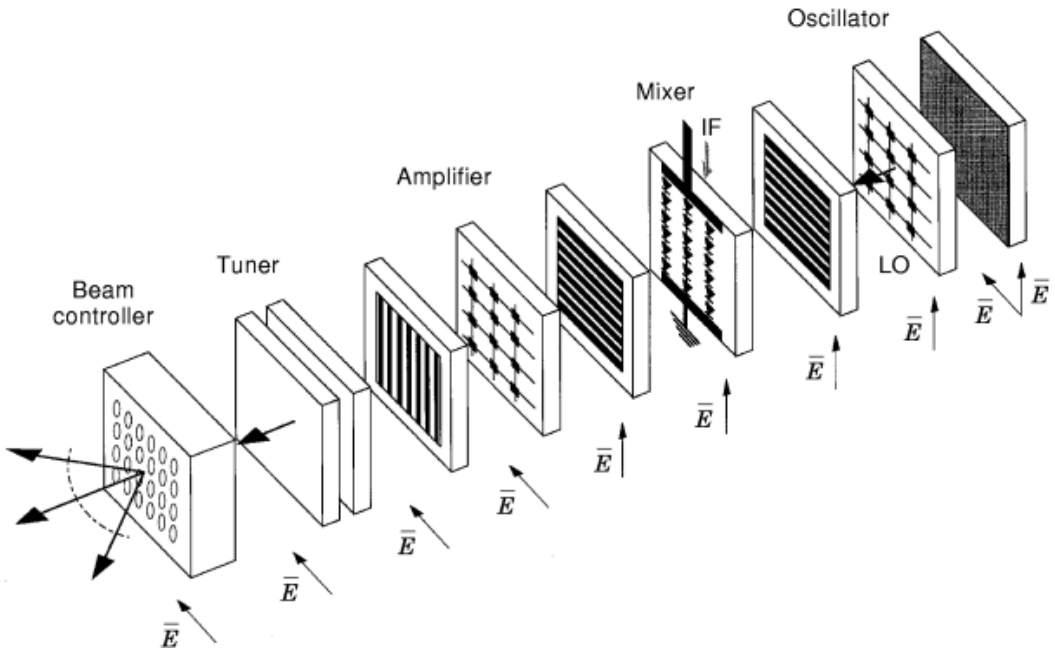


**Fig. 17.** Quasi-optical transceiver front end consisting of cascaded quasi-optical arrays. Figure courtesy of J. C. Chiao, University of Hawaii.

devices, including their use in Gaussian-beam waveguide systems. Frequency-dependent components include path-length modulators, polarization processing components, polarization transducers, hybrids, attenuators, power dividers, ferrite devices, absorbers, and calibration loads. Frequency-dependent components include planar frequency-selective surfaces and grids, perforated plates, interferometers, layered dielectrics, diffraction gratings, and resonators.

## Quasi-Optical Subsystems and Modeling Techniques

One of the attractive features of the quasi-optical approach is the ability to form systems by cascading surfaces that perform different analog signal-processing functions, such as the transceiver front end shown in Fig. 17. Numerous individual components have already been developed, and a demonstration of an end-to-end quasi-optical subsystem could occur soon.

To characterize the various components that comprise a quasi-optical subsystem, one must understand the complicated interactions among the semiconductor devices, the antenna element, dielectric substrate, and the radiated and evanescent fields. Determining the driving-point impedance presented to the device at each feed point of the array is thus a nontrivial task. Further complications arise from edge effects and the mutual coupling between array elements. One of the simplest techniques for making this problem more tractable is to assume an infinite array with identical cells. Based on symmetry, a unit cell can be defined with prescribed boundary conditions.

An example of a transmission-line model arising from this approximation is that of a diode-loaded grid shown in Fig. 18 (45). The vertical metal leads of the grid are represented by a shunt inductor, and the substrate is represented by a section of transmission line whose characteristic impedance is equal to the wave impedance in the dielectric. A system such as the one in Fig. 17 can be characterized in a similar manner by cascading

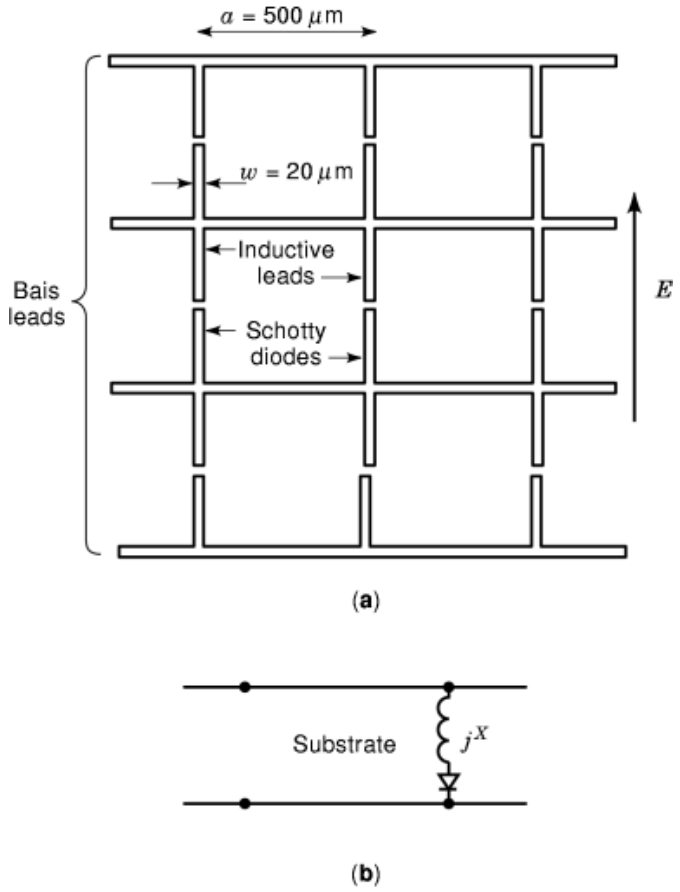


**Fig. 18.** (a) Diode-loaded grid and (b) equivalent transmission-line model (45). Courtesy IEEE.

equivalent transmission-line models. For more complex array geometries, full-wave methods must be used to more accurately design these systems.

For a more detailed discussion of quasi-optical circuits, the interested reader is referred to Ref. 1.

## BIBLIOGRAPHY

1. R. A. York Z. B. Popović (eds.) *Active and Quasi-Optical Arrays for Solid-State Power Combining*, New York: Wiley, 1997.
2. K. Chang C. Sun Millimeter-wave power-combining techniques, *IEEE Trans. Microw. Theory Tech.*, **MTT-31**: 91–107, 1983.
3. J. W. Mink Quasi-optical power combining of solid-state millimeter-wave sources, *IEEE Trans. Microw. Theory Tech.*, **34**: 273–279, 1986.
4. Z. B. Popović *et al.* Bar-grid oscillators, *IEEE Trans. Microw. Theory Tech.*, **38**: 225–230, 1990.
5. Z. B. Popović *et al.* A 100-MESFET planar grid oscillator, *IEEE Trans. Microw. Theory Tech.*, **39**: 193–200, 1991.
6. R. M. Weikle, II *et al.* Planar MESFET grid oscillators using gate feedback, *IEEE Trans. Microw. Theory Tech.*, **39**: 193–200, 1991.

7. J. B. Hacker *et al.* A 10-watt X-band grid oscillator, *IEEE MTT-S Int. Microw. Symp. Dig.*, San Diego, CA, 1994, pp. 823–826.
8. S. C. Bundy Z. B. Popović A generalized analysis for grid oscillator design, *IEEE Trans. Microw. Theory Tech.*, **42**: 2486–2491, 1994.
9. P. Preventza M. Matloubian D. B. Rutledge A 43-GHz AlInAs/GaInAs/InP HEMT grid oscillator, *IEEE MTT-S Int. Microw. Symp. Dig.*, Denver, CO, 1997, pp. 1057–1060.
10. W. A. Shiroma Z. Popović Analysis and optimization of grid oscillators, *IEEE Trans. Microw. Theory Tech.*, **45**: 2380–2386, 1997.
11. W. A. Shiroma B. L. Shaw Z. B. Popović A 100-transistor quadruple grid oscillator, *IEEE Microw. Guided-Wave Lett.*, **4**: 350–351, 1991.
12. T. Mader S. Bundy Z. B. Popović Quasi-optical VCOs, *IEEE Trans. Microw. Theory Tech.*, **41**: 1775–1781, 1993.
13. K. D. Stephan Inter-injection-locked oscillators for power combining and phased arrays, *IEEE Trans. Microw. Theory Tech.*, **34**: 1017–1025, 1986.
14. R. A. York R. C. Compton Mode-locked oscillator arrays, *IEEE Microw. Guided-Wave Lett.*, **1**: 215–218, 1991.
15. J. Birkeland T. Itoh A 16 element quasi-optical FET oscillator power combining array with external injection locking, *IEEE Trans. Microw. Theory Tech.*, **40**: 475–481, 1992.
16. M. J. Vaughan R. C. Compton 28 GHz omni-directional quasi-optical transmitter array, *IEEE Trans. Microw. Theory Tech.*, **43**: 2507–2509, 1995.
17. A. Mortazawi B. C. DeLoach A nine-MESFET two-dimensional power combining array employing an extended resonance technique, *IEEE Microw. Guided-Wave Lett.*, **3**: 214–216, 1993.
18. R. A. York R. C. Compton Quasi-optical power combining using mutually synchronized oscillator arrays, *IEEE Trans. Microw. Theory Tech.*, **39**: 1000–1009, 1991.
19. R. A. York Nonlinear analysis of phase relationships in quasi-optical oscillator arrays, *IEEE Trans. Microw. Theory Tech.*, **41**: 1799–1809, 1993.
20. J. Lin S. T. Chew T. Itoh A unilateral injection-locking type active phased array for beam scanning, *IEEE MTT-S Int. Microw. Symp. Dig.*, San Diego, CA, 1994, pp. 1231–1234.
21. F. Poegel *et al.* Demonstration of an oscillating quasi-optical sab power combiner, *IEEE MTT-S Int. Microw. Symp. Dig.*, Orlando, FL, 1995, pp. 917–920.
22. K. D. Stephan W. A. Morgan Analysis of inter-injection-locked oscillators for integrated phased arrays, *IEEE Trans. Antennas Propag.*, **35**: 771–781, 1987.
23. P. Liao R. A. York A new phase-shifterless beam scanning technique using arrays of coupled oscillators, *IEEE Trans. Microw. Theory Tech.*, **41**: 1810–1815, 1993.
24. P. Liao R. A. York A 1-watt X-band power-combining array using coupled VCOs, *IEEE MTT-S Int. Microw. Symp. Dig.*, San Diego, CA, 1994, pp. 1235–1238.
25. M. Gouker Spatial power combining, in R. A. York and Z. B. Popović (eds.), *Active and Quasi-Optical Arrays for Solid-State Power Combining*, New York: Wiley, 1997, Chap. 2.
26. M. Kim *et al.* A grid amplifier, *IEEE Microw. Guided Wave Lett.*, **1**: 322–324, 1991.
27. M. Kim *et al.* A 100-element HBT grid amplifier, *IEEE Trans. Microw. Theory Tech.*, **41**: 1762–1771, 1993.
28. M. P. De Lisio *et al.* Modelling and performance of a 100-Element pHEMT grid amplifier, *IEEE Trans. Microw. Theory Tech.*, **44**: 2136–2144, 1996.
29. C.-M. Liu *et al.* Monolithic 40-GHz 670-mW HBT grid amplifier, *IEEE MTT-S Int. Microw. Symp. Dig.*, San Francisco, CA, 1996, pp. 1123–1126.
30. M. P. De Lisio *et al.* A 44-60 GHz monolithic pHEMT grid amplifier, *IEEE MTT-S Int. Microw. Symp. Dig.*, San Francisco, CA, 1996, pp. 1127–1130.
31. H. S. Tsai M. J. W. Rodwell R. A. York Planar amplifier array with improved bandwidth using folded-slots, *IEEE Microw. Guided Wave Lett.*, **4**: 112–114, 1994.
32. H. S. Tsai R. A. York Quasi-optical amplifier array using direct integration of MMICs and 50-Ω multi-slot antenna, *IEEE MTT-S Int. Microw. Symp. Dig.*, Orlando, FL, 1995, pp. 593–596.
33. J. S. H. Schoenberg S. C. Bundy Z. B. Popović Two-level power combining using a lens amplifier, *IEEE Trans. Microw. Theory Tech.*, **42**: 2480–2485, 1994.
34. J. Schoenberg *et al.* Quasi-optical antenna array amplifiers, *IEEE MTT-S Int. Microw. Symp. Dig.*, Orlando, FL, 1995, pp. 605–608.

35. S. Hollung A. Cox Z. Popović A bi-directional quasi-optical lens amplifier, *IEEE Trans. Microw. Theory Tech.*, **45**: 2352–2357, 1997.
36. T. Ivanov A. Mortazawi A two stage spatial amplifier with hard horn feeds, *IEEE Microw. Guided Wave Lett.*, **6**: 88–90, 1996.
37. C.-Y. Chi G. M. Rebeiz A quasi-optical amplifier, *IEEE Microw. Guided Wave Lett.*, **3**: 164–166, 1993.
38. N.-S. Cheng *et al.* 20 watt spatial power combiner in a waveguide, *IEEE MTT-S Int. Microw. Symp.*, Baltimore, MD, 1998, pp. 1457–1460.
39. E. A. Sovero *et al.* A Ka band monolithic quasi optic amplifier, *IEEE MTT-S Int. Microw. Symp.*, Baltimore, MD, 1998, pp. 1453–1456.
40. C. F. Jou *et al.* Millimeter-wave diode frequency doubler, *IEEE Trans. Microw. Theory Tech.*, **36**: 1507–1514, 1988.
41. H.-X. L. Liu *et al.* Monolithic quasi-optical frequency tripler array with 5-W output power at 99 GHz, *IEEE Electron Devices Lett.*, **14**: 329–331, 1993.
42. A. Moussessian *et al.* A terahertz grid frequency doubler, *IEEE MTT-S Int. Microw. Symp. Dig.*, Denver, CO, 1997, pp. 683–686.
43. D. S. Kurtz *et al.* Submillimeter-wave sideband generation using a planar diode array, *IEEE MTT-S Int. Microw. Symp.*, Baltimore, MD, 1998, pp. 1903–1906.
44. J. B. Hacker *et al.* A 100-element planar Schottky diode grid mixer, *IEEE Trans. Microw. Theory Tech.*, **40**: 557–562, 1992.
45. W. W. Lam *et al.* Millimeter-wave diode-grid phase shifters, *IEEE Trans. Microw. Theory Tech.*, **36**: 902–907, 1988.
46. L. B. Sjögren *et al.* Phased array operation of a diode grid impedance surface, *IEEE Trans. Microw. Theory Tech.*, **42**: 565–572, 1994.
47. X. H. Qin *et al.* Monolithic millimeter-wave beam control array, *IEEE MTT-S Int. Microw. Symp. Dig., Orlando, FL*, 1995, pp. 1669–1672.
48. K. D. Stephan F. H. Spooner P. F. Goldsmith Quasi-optical millimeter-wave hybrid and monolithic PIN-diode switches, *IEEE Trans. Microw. Theory Tech.*, **41**: 1791–1798, 1993.
49. J.-C. Chiao D. B. Rutledge Microswitch beam-steering grid, *17th Int. Conf. Infrared Millimeter Waves Dig., Pasadena, CA*, 1992, pp. 406–407.
50. M .A. Gouker Toward standard figures-of-merit for spatial and quasi-optical power-combined arrays, *IEEE Trans. Microw. Theory Tech.*, **43**: 1614–1617, 1995.
51. D. R. Gagnon Highly sensitive measurements with a lens-focused reflectometer, *IEEE Trans. Microw. Theory Tech.*, **39**: 2237–2240, 1991.
52. P. F. Goldsmith *Quasioptical Systems*, New York: IEEE Press, 1998.
53. R. A. York P. Liao J. J. Lyrch Oscillator array dynamics with broadband N-port coupling networks, *IEEE Trans. Microw. Theory Tech.*, **42**: 2040–2045, 1994.

WAYNE A. SHIROMA
MICHAEL P. DE LISIO
University of Hawaii at Manoa